Acta Biomed 2021; Vol. 92, Supplement 5: e2021406 DOI: 10.23750/abm.v92iS5.11870

Original article

Diagnostic performance of DIXON sequences on low-field scanner for the evaluation of knee joint pathology

Flavia Cobianchi Bellisari[1], Federico Bruno[1,2], Riccardo Monti[1], Claudia Cicerone[1], Pierpaolo Palumbo[1,2], Francesco Arrigoni[1], Silvia Mariani[1], Camilla Gianneramo[1], Maria Luisa Mangoni di S. Stefano[3], Mattia Carbone[4], Francesco Gentili[5], Maria Antonietta Mazzei[6], Carlo Masciocchi[1], Antonio Barile[1]

[1]Department of Biotechnological and Applied Clinical Sciences, University of L'Aquila, L'Aquila, Italy; [2]Italian Society of Medical and Interventional Radiology (SIRM), SIRM Foundation, Milan, Italy; [3]Dipartimento di Laboratorio di Analisi e dei Servizi, Azienda Sanitaria Locale Napoli 3 Sud, Napoli, Italy; [4]Department of Radiology, San Giovanni E Ruggi D'Aragona Hospital, Salerno, Italy; [5]Section of Radiology, Unit of Surgical Sciences, University of Parma, Parma, Italy; [6]Department of Medical, Surgical and Neuro Sciences, University of Siena, Department of Radiological Sciences, Unit of Diagnostic Imaging, Azienda Ospedaliera Universitaria Senese, Siena, Italy

Abstract. *Background and aim:* Recently, there has been a growing interest in the use of Dixon sequence for knee MRI in order to save time spent on the scanner, and improving diagnostic utility. Our purpose was to compare the diagnostic performance of Dixon sequence on low-field MRI with the proton-density sequence on high-field MRI. *Methods:* This prospective study included 40 patients who underwent 0.25T knee MRI, using the routine protocol with the addition of a sagittal 4-point Dixon sequence (SPED), and an additional sequence on 1.5T scanner, consisting in a fat-suppressed proton-density fast-spin-echo (FS PD-FSE). Two radiologists independently examined the images, evaluating the anatomic identification score and diagnostic performances of the two sequences. Interreader agreement was evaluated using an intraclass correlation coefficient (ICC). *Results:* Final population counted 34 patients (36 knee MR images) with a mean age of 52.9 years (range, 18–75 years). Interreader agreement was very high except for cartilage injuries at medial femoral condyle and medial tibial plateau (ICC SPED: 0.757, ICC FS PD-FSE: 0.746), even if not statistically significant. There were no significant differences in mean signal-to-noise ratio (SNR), artifacts presence and diagnostic confidence between SPED and PD-FS sequence. *Conclusions*: Dixon sequences on low-field scanner have a comparable diagnostic accuracy to PD-FS sequence obtained on a high field scanner for knee MR imaging. (www.actabiomedica.it)

Key words: Dixon, knee MRI, low-field MR, SPED

Introduction

Since the early 1980s, magnetic resonance imaging (MRI) has increasingly become essential for the non-invasive diagnosis and treatment planning of musculoskeletal conditions, thanks to its excellent soft-tissue contrast and multiparametric features (1-12). Knee joint studies are among the most frequent imaging examinations performed in daily practice, given the high incidence of derangements affecting both the young and aging population (5, 8, 9, 11, 13-17). MRI is used to assess all knee structures' integrity, including the articular cartilage, ligaments, and menisci (1, 9, 10, 18-22). MRI knee protocol and sequences should ensure the detection of both soft tissue and osseous structures with high detail and accuracy (23). Most centers perform imaging examinations on high-field scanners (1-3T); however, especially in MSK radiology,

imaging at low field strengths (<1T) using small, low-cost, easily installed scanners, has demonstrated excellent diagnostic accuracy (24). One of the limitations of low-field systems is the technical inability to obtain fat-saturated proton density (FS PD-FSE) sequences (25). The Dixon technique can suppress fat with less metal artifacts than chemical fat saturation images, and compensate for B0 field inhomogeneities caused by the open configuration magnets (26).

Many studies have documented the ability of the Dixon multi-point technique in detecting anatomic structures in MSK imaging, reducing the acquisition time in high field and very-high field systems (>1.5-3T) (27).

The purpose of this study is to compare the diagnostic performance of a low field (LF) 4-point Dixon sequence (SPED, spin echo double echo Dixon) to a standard high field (HF) PD sequence at 1.5T in knee imaging.

Material and Methods

Patient Population

We evaluated 40 consecutive patients who underwent knee MRI imaging on a 0.25T permanent magnet MR system (G-Scan, Esaote, Genova, Italy) with indications for traumatic, inflammatory, and degenerative knee disorders. Exclusion criteria were age under 18 years, history of cancer, and absence of joint pathology; six patients were excluded and the final study population included 36 joints in 34 patients (mean age, 52.9 years; range, 18–75 years), as two patients had bilateral scans. These patients were submitted on the same day to an additional knee MRI scan at high-field scanner (1.5T).

Written informed consent was obtained from all patients who participated in this study.

MRI Protocol

All exams performed on the low field machine (0.25T G-Scan, Esaote, Genova, Italy) were performed with patients in supine position with the knee slightly flexed, using a knee-dedicated coil. The imaging protocol included axial T2 FSE, coronal T2 FSE, sagittal T2 FSE, sagittal T1 FSE, and a sagittal SPED sequence (TR 1400, TE 25-39, NEX 1, FOV 21.0, THK 4, spacing gap 0.4; matrix 288·224; time of execution 5 minutes and 18 seconds).

The high-field scan (1.5 T Signa Horizon, GE Healthcare, Chicago, Illinois USA) included a sagittal FSE PD-FS (TR 1525, TE 16.5, NEX 2; FOV 18.0, THK 4, spacing gap 0.4, matrix 288·224; time of execution 2 minutes and 20 seconds).

Imaging parameters are summarized in Table 1.

Image analysis

LF and HF sequences were separated and anonymized. Cases were reviewed in two reading

Table 1. Imaging parameters for MRI sequences

Imaging parameter	Sagittal SPED	Sagittal FSE PD- FS
Field strength	0.25T	1.5T
TR (ms)	1400	1525
TE (ms)	IP 25	16.5
	FO 32	
	WO 32.1	
	OP 39	
NEX	1	2
FOV (mm)	4	4
Gap (mm)	0.4	0.4
Matrix	288x224	288x224

periods, ensuring a minimum of 4 weeks between the start of each period. A different random reading order containing both LF and HF studies was created for each reader and reading period. LF and HF images from the same patient were never read in the same reading period. Two musculoskeletal radiologists with 6 and 27 years of experience, respectively, independently reviewed the cases.

Sagittal SPED and FS PD-FSE sequences were compared, and the anatomic structures were graded as follows:

- Meniscus (medial and lateral): intact (normal, degenerative changes without tear, post-surgical changes without tear), definite tear (increased signal reaching the articular surface on at least two slices or morphologic deformity).

- Posterior cruciate ligament: intact, partial tear (thickening and increased signal of the ligament and/or partial disruption of fibers), complete tear (complete disruption of all fibers).

- Anterior cruciate ligament: intact, partial tear (thickening and increased signal of the ligament and/or partial disruption of fibers), complete tear (complete disruption of all fibers).

- Articular cartilage (four articular surfaces: medial and lateral femoral condyles, medial and lateral tibial plateaus. Adapted from the ICRS classification.): normal, low-grade chondropathy (signal abnormality including increased signal intensity, dark lines, chondral defect/fissure < 50% thickness of the cartilage) and high-grade chondropathy (chondral defect/fissure > 50% thickness of the cartilage, or defect extending through the subchondral bone plate). Osteochondritis dissecans lesions and osteochondral injuries were categorized as high-grade defects.

- Bone/marrow (fracture, contusion, or stress change; marrow replacing disease): present or absent.

- Synovia and joint effusion were graded collectively in terms of the estimated maximal distention of the synovial cavity: grade 0 (normal), grade 1 (<33% of maximum potential distention); grade 2 (33%–66% of maximum potential distention), grade 3 (>66% of maximum potential distention).

- Additional comments, including callbacks for poor image quality related to artifacts, poor SNR, and diagnostic confidence (subjectively graded 0 to 5 points).

Interobserver agreement between the radiologists was analyzed using an intraclass correlation coefficient (ICC). ICC values ≤0.40 indicated poor agreement, whereas ICC values of 0.40–0.75 indicated fair-to-good agreement, and values 0.75 indicated excellent agreement.

Results

Detailed intra-class coefficient (ICC) values for each region are summarized in Table 2. In particular, we found excellent ICC values for both images in all structures, except for medial femoral condyle and medial tibial plateau (0.757 and 0.746, respectively), even if

Table 2. Results of ICC between SPED and FSE PD-FS. Data are means with 95% confidence intervals in parentheses. MM medial meniscus, LM lateral meniscus, MFC medial femoral condyle, LFC lateral femoral condyle, MTP medial tibial plateau, LTP lateral tibial plateau

	SPED	FSE PD-FS	p-value
MM	0.972 (0.912-0.986)	0.912(0.856-0.978)	0.423
LM	0.967 (0.768-0.963)	0.930 (0.896-0.954)	0.135
Bone	0.934 (0.923-0.987)	0.970 (0.879-0.997)	0.158
MFC	0.757 (0.820-0.934)	0.942 (0.932-0.953)	0.224
LFC	0.921 (0.866-0.984)	0.934 (0.865-0.967)	0.156
MTP	0.746 (0.790-0.810)	0.876 (0.857-0.965)	0.135
LTP	0.950 (0.897-0.980)	0.931 (0.876-0.985)	0.224
Synovitis	0.879 (0.965-0.981)	0.856 (.0.765-0.934)	0.341

not statistically significant. Examples of 0.25 and 1.5 T MR knee images demonstrating ligament, meniscal, and osteochondral lesions are shown in Figure 1-3.

Mean SNR was 3.6 for SPED and 3.8 for FS PD-FSE, respectively, without statistically significant difference (p=0.235).

Artifact presence was slightly higher in FS PD-FSE than SPED, however without reaching significance (0.8 and 0.6 respectively, p=0.121) (figure 4).

Table 3 summarizes scores on SPED and FS-PD-FSE images in terms of artefacts, mean SNR and diagnostic confidence.

Concerning the final diagnosis, out of a total of 36 knees examined, 9 cases had cruciate ligament injury: 7 cases of complete tear of anterior cruciate ligament, 2 cases of complete tear of the posterior cruciate ligament. Thirty patients had cartilage injuries: 22 cases of cartilage injuries at the medial femoral condyle or medial tibial plateau, 8 cases at lateral femoral condyle or lateral tibial plateau. Thirty-four cases of meniscal tears: 25 of medial meniscus root and 9 of the lateral meniscus. 18 cases of synovitis and 12 cases of bone marrow edema.

Discussion

Since it was first introduced in the field of medical imaging in the early 1980s, MRI has become essential for the whole-body non invasive imaging diagnosis and therapy of multiple different pathologic conditions (9, 13, 19, 21, 28-41). In MSK imaging – and particularly the knee - since the 1990s, when compared to the arthroscopic reference standard, MRI has repeatedly demonstrated high accuracy, especially in the diagnosis of fibrocartilage and ligament pathology (8, 9, 22, 42-47).

Few publications have evaluated the efficacy of low-field MRI compared to arthroscopy. Lee et al. reported that low-field extremity MRI scanners accurately identify tears of the medial meniscus and anterior cruciate ligament and that MRI can be useful for quantifying extension of knee pathology, regardless of low or high field (48). Lokannavar et al. demonstrated that the accuracy of MRI was 97.9% for the medial meniscus, 97.2% for the lateral meniscus, 97.9% for the anterior cruciate ligament, and 99.32% for the posterior cruciate ligament (49).

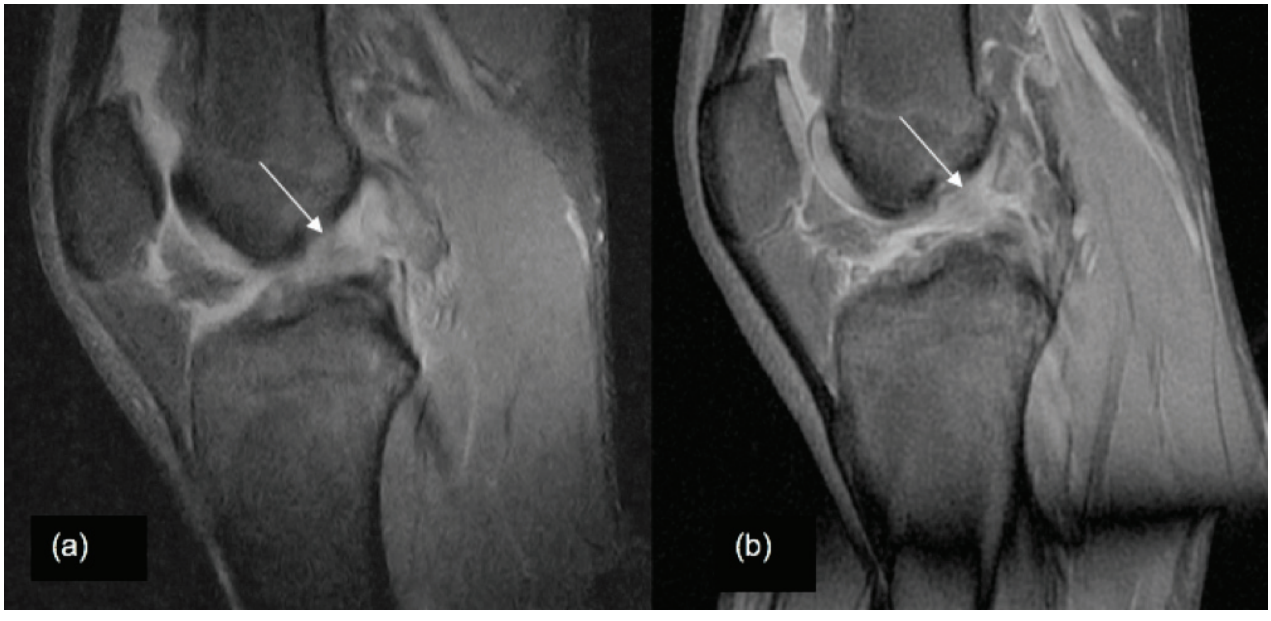

Figure 1. Anterior cruciate ligament tear. (A) Sagittal view of 0.25-T SPED and (B) 1.5-T FS PD-FSE knee images demonstrating anterior cruciate ligament tear (arrows).

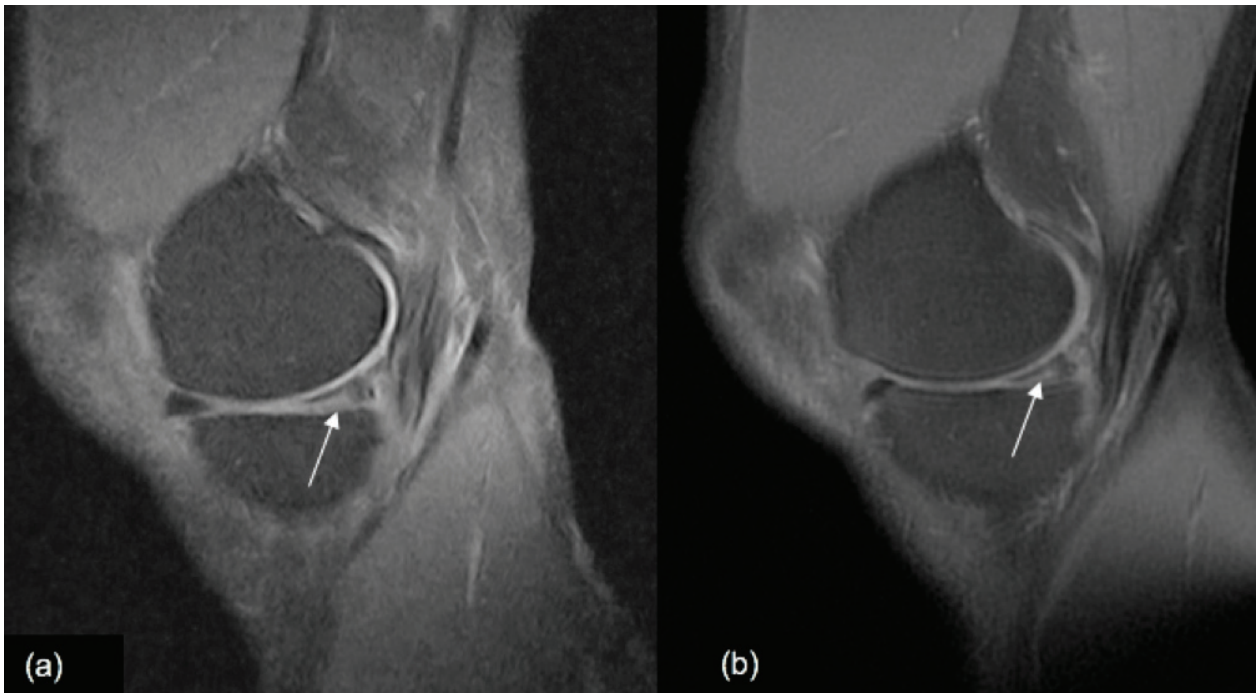

Figure 2. Medial meniscus tear. (A) Sagittal view of 0.25-T SPED and (B) 1.5-T FS PD-FSE knee images demonstrating medial meniscus tear (arrows).

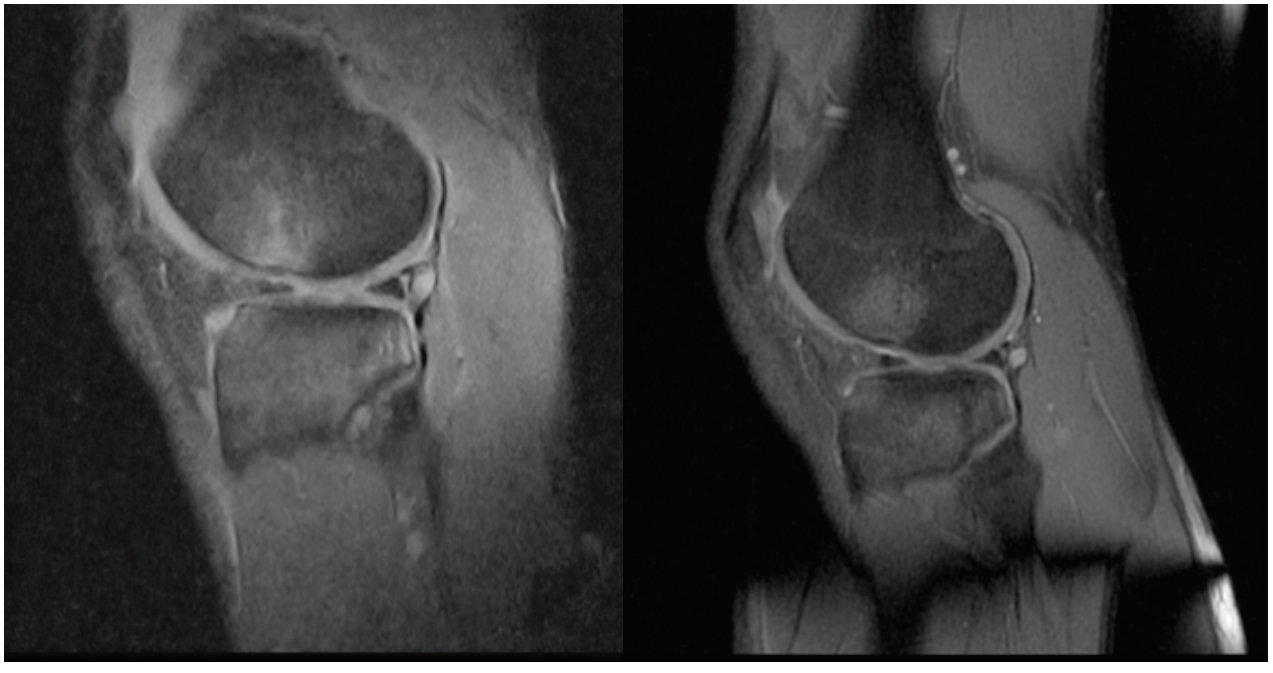

Figure 3. Bone contusion. (A) Sagittal view of 0.25-T SPED and (B) 1.5-T FS PD-FSE knee images demonstrating bone contusion of the lateral femoral condyle (arrows).

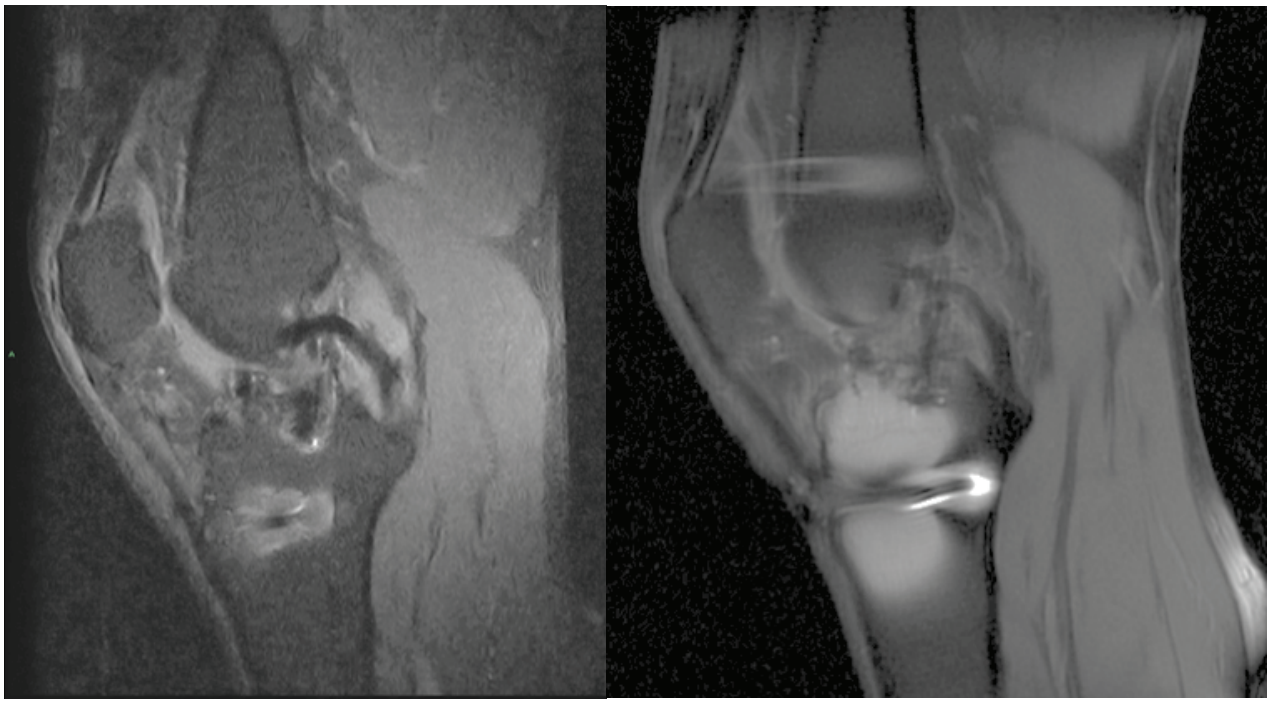

Figure 4. Metal artifacts. (A) Sagittal view of 0.25-T SPED and (B) 1.5-T FS PD-FSE knee images demonstrating the chemical saturation failed near the metal implants (arrows). The image distortion in SPED is more limited, giving an important advantage to the SPED sequence. There was no significant difference in diagnostic confidence between the two images (p=0.347).

Table 3. Artifacts, mean signal-to-noise ratio (SNR), and diagnostic confidence

	Artifacts	**SNR**	**Diagnostic confidence**
SPED	0.6 (0-1)	3.6 (0-5)	3.8 (0-5)
FS PD-FSE	0.8 (0-1)	3.7 (0-5)	4.1 (0-5)
p-value	0.121	0.235	0.347

Previous literature agrees upon the diagnostic performance of high and low-field MRI, although they do not have the same image quality. In 2007, Ghazinoor and colleagues provided an overview of the different available extremity scanners and their use in the diagnostic examination of upper and lower extremities (24). They confirmed that both meniscal and ligamentous injuries/tears are very well detected and highlight the sensitivity of IR images for bone-marrow contusions. They agreed with literature findings that cartilage abnormalities, especially low-grade pathology, are more difficult to evaluate on low-field scans, demonstrating the relevance of the experience and training of radiologists in the identification of musculoskeletal pathology (50, 51).

A major limitation of low field systems is the technical impossibility to obtain PD-FS sequences (52).

The open configuration magnets, used by low-field permanent magnets, have - as a trade-off - a lower signal-to-noise ratio. Limitations in the signal-to-noise ratio may necessitate longer imaging times or result in restricted spatial resolution and the inability to use frequency-selective and chemical shift fat saturation (53).

Fat-suppression techniques are frequently used in MR imaging of the musculoskeletal system to extend the dynamic range of tissue contrast, and fat suppression may be beneficial in imaging articular cartilage. Dixon techniques alternatively can suppress fat with

less metal artifact than seen in chemical fat saturation images. Moreover, sequences with a shorter TE, such as T1 or PD weighted sequences, will typically also demonstrate fewer artifacts than sequences with a longer TE, and thus PD sequences are beneficial as they produce minimal artifacts (54). This imaging technique provides chemical shift-separated fat and water images to quantify the fat amount (53). The multi-point Dixon technique using the phase difference between fat and water signals allows a flexible echo time and sequence design, compensating for B0 field heterogeneity and producing homogeneous fat and water separation. Furthermore, it rapidly generates multiple images (including fat-saturated and T2-like images, in-phase) in a single acquisition (53-55).

Many studies documented the ability of the Dixon multi-point technique in detecting anatomic structures reducing the acquisition time in Ultra High Field systems (UHF, 3 T) (56). Low et al. reported that mDixon (three-point) water only is superior to the STIR image for quality image, equal for homogeneity in fat saturation and is less subject to motion and metal artifact (57). Park and colleagues demonstrated that mDixon, providing simultaneous acquisition of T2 weighted images with and without FS, can reduce the scan time for knee joint MRI by approximately 27%. Their anatomic identification abilities and diagnostic performance are comparable with that of FSE T2 for meniscal, cartilage, and ligament injuries of the knee joint (54). In a recent study, Bastian-Jordan and colleagues evaluated the effect on diagnostic image quality and acquisition time utilizing a novel 2-point Dixon sequence to replace two standard PD-FS sequences in routine MRI evaluation of the knee. They documented no loss in diagnostic confidence and a superior fat saturation across the majority of cases, as Dixon techniques usually produce a higher signal to noise than standard sequences due to insensitivities to B0/B1 field inhomogeneities (26).

Our diagnostic center was recently provided a pre-release version of a 4-point Dixon sequence for our 0.25 T Esaote G-Scan system. This sequence is called SPED and it is a spin echo double echo, acquired by the Dixon method, which generates four final images: opposite-phase, in-phase, water only, and fat only. To the best our knowledge, there are few previous reports on the applications of the Dixon method in low field image systems for MSK knee imaging.

Our study aimed to compare the diagnostic performance of the LF SPED knee MRI protocol, consisting of four multi-planar sequences including a sagittal SPED (spin echo Dixon), to that of our standard HF protocol.

The results of our study have demonstrated that the SPED sequence is comparable to high field PD-FS sequences. In particular, the interreader agreement on the SPED protocol was interchangeable with the standard PD –FS sequences for all of the evaluated structures, with no significant disagreement when using SPED images. These results are in line with a previous comparison of standard and Dixon sequences conducted by Park et al. on 3T system (interreader agreement 0.754-0.883) (53, 54).

Frequency of readers being able to detect significant knee pathology using SPED and PD–FS protocols was also not significantly different, except that more high-grade chondral lesions were reported on standard HF PD-FS images.

The diagnostic content of the MR images obtained at 0.25T and 1.5T was equivalent. The same diagnoses were made on either systems, and there was no significant difference in diagnostic confidence.

Although the SNR was better for the 1.5T system, the overall image quality was comparable and anatomic structures were well defined on both systems.

We registered several image artifacts in both sequences. In particular, in SPED sequences, the main artifacts were due to magic angle phenomenon; global evaluation of the exam with other protocol sequences didn't affect the diagnostic confidence for the final diagnosis.

We found that SPED was less sensitive to artifacts due to magnetic field inhomogeneity for the presence of metallic foreign bodies. This is related both to the intrinsic characteristics of the SPED sequence and the lower magnetic field intensity.

Since the Dixon method is less sensitive to magnetic field inhomogeneity than PD-FS, it can achieve excellent fat–water separation, also in cases with metallic foreign bodies. For this reason, it can be valuable in the post-surgical evaluation for patients with metal devices.

Our study has two important limitations. First, a relatively small number of patients were evaluated. Second, we did not include a comparison with arthroscopic evaluation. However, there is abundant demonstration of low field MRI diagnostic accuracy compared to arthroscopic gold standard in literature.

The main advantages of extremity-dedicated LF MR scanners are low purchase and maintenance costs. In a previous study, Vellet estimated the purchase and installation costs of a 1.5 T MR scanner to be 2.7 times higher than the costs of a LF scanner. The maintenance costs of a 0.3 T MR scanner are about 37% lower compared to a 1.5 T scanner (58).

Furthermore, as radiology departments attempt to scan more patients in less time, sequence optimization becomes critical, and Dixon-based approaches are potentially very useful in this regard.

In conclusion, the Dixon method, which has already been validated and compared to FS PD-FSE sequence in high field MR scanners, can also be feasible at LF scanners.

The ability to perform low field SPED sequence without compromising the diagnostic value may have significant clinical advantages, including increased efficiency of and access to MRI and possible improved patient comfort and decreased motion artifacts.

Conflict of Interest: Each author declares that he or she has no commercial associations (e.g. consultancies, stock ownership, equity interest, patent/licensing arrangement etc.) that might pose a conflict of interest in connection with the submitted article

References

1. Zoccali C, Arrigoni F, Mariani S, Bruno F, Barile A, Masciocchi C. An unusual localization of chondroblastoma: The triradiate cartilage; from a case report a reconstructive technique proposal with imaging evolution. J Clin Orthop Trauma 2017; 8: S48-S52.
2. Zappia M, Castagna A, Barile A, Chianca V, Brunese L, Pouliart N. Imaging of the coracoglenoid ligament: a third ligament in the rotator interval of the shoulder. Skeletal Radiol 2017; 46: 1101-11.
3. Salvati F, Rossi F, Limbucci N, Pistoia ML, Barile A, Masciocchi C. Mucoid metaplastic-degeneration of anterior cruciate ligament. J Sports Med Phys Fitness 2008; 48: 483-7.
4. Masciocchi C, Lanni G, Conti L, et al. Soft-tissue inflammatory myofibroblastic tumors (IMTs) of the limbs: potential and limits of diagnostic imaging. Skeletal Radiol 2012; 41: 643-9.
5. Mariani S, La Marra A, Arrigoni F, et al. Dynamic measurement of patello-femoral joint alignment using weight-bearing magnetic resonance imaging (WB-MRI). Eur J Radiol 2015; 84: 2571-8.
6. Di Pietto F, Chianca V, de Ritis R, et al. Postoperative imaging in arthroscopic hip surgery. Musculoskelet Surg 2017; 101: 43-49.
7. Chianca V, Albano D, Messina C, et al. Rotator cuff calcific tendinopathy: from diagnosis to treatment. Acta Biomed 2018; 89: 186-96.
8. Bruno F, Barile A, Arrigoni F, et al. Weight-bearing MRI of the knee: a review of advantages and limits. Acta Biomed 2018; 89: 78-88.
9. Bruno F, Arrigoni F, Palumbo P, et al. New advances in MRI diagnosis of degenerative osteoarthropathy of the peripheral joints. Radiol Med 2019; 124: 1121-27.
10. Bruno F, Arrigoni F, Palumbo P, et al. The Acutely Injured Wrist. Radiol Clin North Am 2019; 57: 943-55.
11. Barile A, Regis G, Masi R, et al. Musculoskeletal tumours: preliminary experience with perfusion MRI. Radiol Med 2007; 112: 550-61.
12. Gentili F, Cantarini L, Fabbroni M, et al. Magnetic resonance imaging of the sacroiliac joints in SpA: with or without intravenous contrast media? A preliminary report. Radiol Med 2019; 124: 1142-50.
13. Silvestri E, Barile A, Albano D, et al. Interventional therapeutic procedures in the musculoskeletal system: an Italian Survey by the Italian College of Musculoskeletal Radiology. Radiol Med 2018; 123: 314-21.
14. Zappia M, Reginelli A, Russo A, et al. Long head of the biceps tendon and rotator interval. Musculoskelet Surg 2013; 97 Suppl 2: S99-108.
15. Piccolo CL, Galluzzo M, Trinci M, et al. Lower Limbs Trauma in Pediatrics. Semin Musculoskelet Radiol 2017; 21: 175-83.
16. Piccolo CL, Galluzzo M, Ianniello S, et al. Pediatric musculoskeletal injuries: role of ultrasound and magnetic resonance imaging. Musculoskelet Surg 2017; 101: 85-102.
17. Marchesoni A, D'Angelo S, Anzidei M, et al. Radiologist-rheumatologist multidisciplinary approach in the management of axial spondyloarthritis: a Delphi consensus statement. Clin Exp Rheumatol 2019; 37: 575-84.
18. Corsini F, Marchetto G, Candeo F, al e. Magnetic resonance study of femorotibial chondropathy with T2* Map sequences. J Radiol Rev 2020; 7: 12-20.
19. Acanfora C, Bruno F, Palumbo P, et al. Diagnostic and interventional radiology fundamentals of synovial pathology. Acta Biomed 2020; 91: 107-15.
20. Bruno F, Arrigoni F, Mariani S, et al. Advanced magnetic resonance imaging (MRI) of soft tissue tumors: techniques and applications. Radiol Med 2019; 124: 243-52.

21. Bruno F, Palumbo P, Arrigoni F, et al. Advanced diagnostic imaging and intervention in tendon diseases. Acta Biomed 2020; 91: 98-106.
22. Cobianchi Bellisari F, Bruno F, Di Murro I, al e. Magnetic resonance imaging and magnetic resonance imaging arthrograph in femoro-acetabular impingement: diagnostic features and retrospective epidemiological evaluation of 4-year experience in a single center. J Radiol Rev 2020; 7: 357-66.
23. Masciocchi C, Conti L, D'Orazio F, Conchiglia A, Lanni G, Barile A, Errors in musculoskeletal MRI, in: Romano L., Pinto A. (Eds.), Errors in Radiology, Springer Milano2012, pp. 209-17.
24. Ghazinoor S, Crues JV, 3rd, Crowley C. Low-field musculoskeletal MRI. J Magn Reson Imaging 2007; 25: 234-44.
25. Guerini H, Omoumi P, Guichoux F, et al. Fat Suppression with Dixon Techniques in Musculoskeletal Magnetic Resonance Imaging: A Pictorial Review. Semin Musculoskelet Radiol 2015; 19: 335-47.
26. Bastian-Jordan M, Dhupelia S, McMeniman M, Lanham M, Hislop-Jambrich J. A quality audit of MRI knee exams with the implementation of a novel 2-point DIXON sequence. J Med Radiat Sci 2019; 66: 163-69.
27. Deligianni X, Bar P, Scheffler K, Trattnig S, Bieri O. High-resolution Fourier-encoded sub-millisecond echo time musculoskeletal imaging at 3 Tesla and 7 Tesla. Magn Reson Med 2013; 70: 1434-9.
28. Scarpino M, Lolli F, Lanzo G, et al. Neurophysiology and neuroimaging accurately predict poor neurological outcome within 24 hours after cardiac arrest: The ProNeCA prospective multicentre prognostication study. Resuscitation 2019; 143: 115-23.
29. Rossi A, Bustini M, Prosperini P, et al. Neuromorphological abnormalities in schizophrenic patients with good and poor outcome. Acta Psychiatr Scand 2000; 101: 161-6.
30. D'Orazio F, Splendiani A, Gallucci M. 320-Row Detector Dynamic 4D-CTA for the Assessment of Brain and Spinal Cord Vascular Shunting Malformations. A Technical Note. Neuroradiol J 2014; 27: 710-7.
31. Barile A, Bruno F, Arrigoni F, et al. Emergency and Trauma of the Ankle. Semin Musculoskelet Radiol 2017; 21: 282-89.
32. Arrigoni F, Bruno F, Zugaro L, et al. Developments in the management of bone metastases with interventional radiology. Acta Biomed 2018; 89: 166-74.
33. Barile A, Quarchioni S, Bruno F, et al. Interventional radiology of the thyroid gland: critical review and state of the art. Gland Surg 2018; 7: 132-46.
34. Cazzato RL, Arrigoni F, Boatta E, et al. Percutaneous management of bone metastases: state of the art, interventional strategies and joint position statement of the Italian College of MSK Radiology (ICoMSKR) and the Italian College of Interventional Radiology (ICIR). Radiol Med 2019; 124: 34-49.
35. Giordano AV, Arrigoni F, Bruno F, et al. Interventional Radiology Management of a Ruptured Lumbar Artery Pseudoaneurysm after Cryoablation and Vertebroplasty of a Lumbar Metastasis. Cardiovasc Intervent Radiol 2017; 40: 776-79.
36. Masciocchi C, Arrigoni F, Ferrari F, et al. Uterine fibroid therapy using interventional radiology mini-invasive treatments: current perspective. Med Oncol 2017; 34: 52.
37. Scialpi M, Cappabianca S, Rotondo A, et al. Pulmonary congenital cystic disease in adults. Spiral computed tomography findings with pathologic correlation and management. Radiol Med 2010; 115: 539-50.
38. Falsetti P, Conticini E, Mazzei MA, et al. Power and spectral Doppler ultrasound in suspected active sacroiliitis: a comparison with magnetic resonance imaging as gold standard. Rheumatology (Oxford) 2021; 60: 1338-45.
39. Arrigoni F, Izzo A, Bruno F, et al. Could anaesthesia be a key factor for the good outcome of bone ablation procedures? A retrospective analysis of a musculoskeletal interventional centre. Br J Radiol 2021; 94: 20200937.
40. Palumbo P, Bruno F, Arrigoni F, et al. Diagnostic and interventional management of infective spine diseases. Acta Biomed 2020; 91: 125-35.
41. Ruscitti P, Berardicurti O, Iacono D, et al. Parenchymal lung disease in adult onset Still's disease: an emergent marker of disease severity-characterisation and predictive factors from Gruppo Italiano di Ricerca in Reumatologia Clinica e Sperimentale (GIRRCS) cohort of patients. Arthritis Res Ther 2020; 22: 151.
42. Vrooijink SH, Wolters F, Van Eck CF, Fu FH. Measurements of knee morphometrics using MRI and arthroscopy: a comparative study between ACL-injured and non-injured subjects. Knee Surg Sports Traumatol Arthrosc 2011; 19 Suppl 1: S12-6.
43. Milewski MD, Sanders TG, Miller MD. MRI-arthroscopy correlation: the knee. Instr Course Lect 2012; 61: 525-37.
44. Liodakis E, Hankemeier S, Jagodzinski M, Meller R, Krettek C, Brand J. The role of preoperative MRI in knee arthroscopy: a retrospective analysis of 2,000 patients. Knee Surg Sports Traumatol Arthrosc 2009; 17: 1102-6.
45. Xix Congresso Nazionale S.I.C.O.O.P. Societa' Italiana Chirurghi Ortopedici Dell'Ospedalita' Privata A, Bruno F, Goderecci R, Barile A, Calvisi V. Comparative evaluation of meniscal pathology: MRI vs arthroscopy. J Biol Regul Homeost Agents 2019; 33: 9-14.
46. Barile A, Conti L, Lanni G, Calvisi V, Masciocchi C. Evaluation of medial meniscus tears and meniscal stability: weight-bearing MRI vs arthroscopy. Eur J Radiol 2013; 82: 633-9.
47. Bruno F, Arrigoni F, Natella R, et al. MR Imaging of the Upper Limb: Pitfalls, Tricks, and Tips. Radiol Clin North Am 2019; 57: 1051-62.
48. Lee YH, Hahn S, Lim D, Suh JS. Articular cartilage grading of the knee: diagnostic performance of fat-suppressed 3D volume isotropic turbo spin-echo acquisition (VISTA) compared with 3D T1 high-resolution isovolumetric examination (THRIVE). Acta Radiol 2017; 58: 190-96.

49. Lokannavar HS, Yang X, Guduru H. Arthroscopic and low-field MRI (0.25 T) evaluation of meniscus and ligaments of painful knee. J Clin Imaging Sci 2012; 2: 24.
50. Panta OB, Neupane NP, Songmen S, Gurung G. Assessment of Knee Joint Injuries with Low Field Strength Magnetic Resonance Imaging. J Nepal Health Res Counc 2016; 14: 89-92.
51. Leigheb M, Guzzardi G, Barini M, et al. Role of low field MRI in detecting knee lesions. Acta Biomed 2018; 90: 116-22.
52. Palosaari K, Tervonen O. Post-processing water-fat imaging technique for fat suppression in a low-field MR imaging system, evaluation in patients with rheumatoid arthritis. MAGMA 2002; 15: 1-9.
53. Park HJ, Lee SY, Rho MH, et al. Usefulness of the fast spin-echo three-point Dixon (mDixon) image of the knee joint on 3.0-T MRI: comparison with conventional fast spin-echo T2 weighted image. Br J Radiol 2016; 89: 20151074.
54. Park HJ, Lee SY, Choi SH, Hong HP, Choi YJ, Kim MS. Reduced metallic artefacts in 3 T knee MRI using fast spin-echo multi-point Dixon compared to fast spin-echo T2-weighted sequences. Clin Radiol 2017; 72: 996 e1-96 e6.
55. He Q, Weng D, Zhou X, Ni C. Regularized iterative reconstruction for undersampled BLADE and its applications in three-point Dixon water-fat separation. Magn Reson Med 2011; 65: 1314-25.
56. Lins CF, Salmon CEG, Nogueira Barbosa MH Applications of the Dixon technique in the evaluation of the musculoskeletal system. Radiol Bras 2021; 54(1):33-42.
57. Low RN, Ma J, Panchal N. Fast spin-echo triple-echo Dixon: initial clinical experience with a novel pulse sequence for fat-suppressed T2-weighted abdominal MR imaging. J Magn Reson Imaging 2009; 30: 569-77.
58. Vellet AD, Lee DH, Munk PL, et al. Anterior cruciate ligament tear: prospective evaluation of diagnostic accuracy of middle- and high-field-strength MR imaging at 1.5 and 0.5 T. Radiology 1995; 197: 826-30.

Correspondence:
Received: 4 June 2021
Accepted: 28 July 2021
Flavia Cobianchi Bellisari, MD
Department of Biotechnological and
Applied Clinical Sciences,
University of L'Aquila, L'Aquila, Italy
E-mail: flavia.cobianchi@gmail.com